Plant Mol Biol (2016) 90:453–466
DOI 10.1007/s11103-016-0429-z

Metal binding to the N-terminal cytoplasmic domain of the P_{IB} ATPase HMA4 is required for metal transport in *Arabidopsis*

Clémentine Laurent[1] · Gilles Lekeux[1] · Ashwinie A. Ukuwela[2] · Zhiguang Xiao[2] · Jean-Benoit Charlier[1] · Bernard Bosman[3] · Monique Carnol[3] · Patrick Motte[1,4] · Christian Damblon[5] · Moreno Galleni[1] · Marc Hanikenne[1,4]

Received: 15 September 2015 / Accepted: 3 January 2016 / Published online: 21 January 2016

Abstract P_{IB} ATPases are metal cation pumps that transport metals across membranes. These proteins possess N- and C-terminal cytoplasmic extensions that contain Cys- and His-rich high affinity metal binding domains, which may be involved in metal sensing, metal ion selectivity and/or in regulation of the pump activity. The P_{IB} ATPase HMA4 (Heavy Metal ATPase 4) plays a central role in metal homeostasis in *Arabidopsis thaliana* and has a key function in zinc and cadmium hypertolerance and hyperaccumulation in the extremophile plant species *Arabidopsis halleri*. Here, we examined the function and structure of the N-terminal cytoplasmic metal-binding domain of HMA4. We mutagenized a conserved CCTSE metal-binding motif in the domain and assessed the impact of the mutations on protein function and localization *in planta*, on metal-binding properties in vitro and on protein structure by Nuclear Magnetic Resonance spectroscopy. The two Cys residues of the motif are essential for the function, but not for localization, of HMA4 *in planta*, whereas the Glu residue is important but not essential. These residues also determine zinc coordination and affinity. Zinc binding to the N-terminal domain is thus crucial for HMA4 protein function, whereas it is not required to maintain the protein structure. Altogether, combining in vivo and in vitro approaches in our study provides insights towards the molecular understanding of metal transport and specificity of metal P-type ATPases.

Keywords Metal P-type ATPase · Metal binding domain · Zinc transport · Structure–function analysis · Arabidopsis

Clémentine Laurent and Gilles Lekeux have contributed equally to this work.

Electronic supplementary material The online version of this article (doi:10.1007/s11103-016-0429-z) contains supplementary material, which is available to authorized users.

✉ Marc Hanikenne
marc.hanikenne@ulg.ac.be

[1] Department of Life Sciences, Center for Protein Engineering (CIP), University of Liège, 4000 Liège, Belgium

[2] School of Chemistry and Bio21 Molecular Science and Biotechnology Institute, University of Melbourne, Parkville, VIC 3010, Australia

[3] Laboratory of Plant and Microbial Ecology, Department of Biology, Ecology, Evolution, University of Liège, 4000 Liège, Belgium

[4] PhytoSYSTEMS, University of Liège, 4000 Liège, Belgium

[5] Chimie Biologique Structurale, Department of Chemistry, University of Liège, Liège, Belgium

Introduction

Zinc is an essential transition metal for development and growth of photosynthetic organisms. It plays important roles as enzyme or structural cofactor in many biochemical processes (Broadley et al. 2007; Palmer and Guerinot 2009; Nouet et al. 2011). However, zinc becomes toxic when present in excess in tissues, through unspecific binding or competition with other metals for the active sites in proteins (Goyer 1997; Gaither and Eide 2001; Hall and Williams 2003; Tuerk and Fazel 2009). To maintain zinc concentration in tissues within an optimal range, plants have developed a complex and tightly controlled zinc homeostasis network. This network relies in part on zinc membrane transporters that ensure zinc uptake, distribution and storage (Krämer et al. 2007; Palmer and Guerinot 2009; Nouet et al. 2011).

In *Arabidopsis thaliana, HMA4* (*Heavy Metal ATPase 4*) encodes a zinc and cadmium efflux pump of the IB subfamily of P-type ATPases (or CPx-ATPases) (Williams and Mills 2005; Palmgren and Nissen 2011; Pedersen et al. 2012; Hanikenne and Baurain 2014) and is an essential node of the metal homeostasis network (Mills et al. 2003; Hussain et al. 2004; Verret et al. 2004). Together with its paralog AtHMA2, the HMA4 transporter is localized at the plasma membrane and is expressed in vascular tissues in roots and shoots (Hussain et al. 2004; Verret et al. 2004; Siemianowski et al. 2013). AtHMA2 and AtHMA4 are responsible for the translocation of zinc from roots to shoots. A *hma2hma4* double *A. thaliana* mutant displays stunted growth resulting from severe zinc deficiency in shoots (Hussain et al. 2004). AtHMA2 and AtHMA4 are also responsible for cadmium translocation to shoots (Wong and Cobbett 2009; Cun et al. 2014). In addition, the HMA4 protein plays a key role in the zinc and cadmium hyperaccumulation and hypertolerance syndrome in the Brassicaceae *Arabidopsis halleri* (Talke et al. 2006; Courbot et al. 2007; Hanikenne et al. 2008, 2013) and *Noccaea caerulescens* (O'Lochlainn et al. 2011; Craciun et al. 2012), an extreme trait enabling these species to colonize metal-polluted soils (Krämer 2010; Hanikenne and Nouet 2011). In *A. halleri*, high expression of *HMA4* supports high rates of root-to-shoot translocation of zinc mediated by xylem loading (Hanikenne et al. 2008). Increased expression of *HMA4* in *A. halleri* results from tandem triplication and *cis*-activation of expression of all three gene copies that were selected for during the evolutionary history of A. halleri (Hanikenne et al. 2008, 2013).

P-type ATPases constitute a superfamily of pumps using the energy of ATP to transport cations, and possibly phospholipids (Kühlbrandt 2004; Palmgren and Nissen 2011). P-type ATPases can be divided into five major classes, I–V, based on ion transport specificities and clustering in phylogenetic trees (Axelsen and Palmgren 1998; Palmgren and Nissen 2011). Despite a low sequence conservation, all P-type ATPases share a set of structural and mechanistic features (Toyoshima and Nomura 2002; Toyoshima and Inesi 2004; Toyoshima 2008, 2009; Palmgren and Nissen 2011). These proteins are characterized by the phosphorylation of an invariant Asp residue by ATP during the ion transport cycle. During this so-called Post-Albers cycle, the pumps undergo a series of conformational changes upon ion binding/release and phosphorylation/dephosphorylation. These conformational changes allow transport of the ion across the membrane. P-type ATPases possess specific cytoplasmic catalytic domains, the Actuator, Nucleotide and Phosphorylation domains, which are essential for the transport cycle. The transmembrane segments (TM) of P-type ATPases constitute the transport domain, which, determines ion selectivity and thanks to a high flexibility, allows binding and release of the ion (Kühlbrandt 2004; Williams and Mills 2005; Palmgren and Nissen 2011).

Proteins of the IB subfamily of P-type ATPases are involved in metal cation transport across membranes (Williams and Mills 2005; Palmgren and Nissen 2011; Pedersen et al. 2012; Hanikenne and Baurain 2014). These proteins possess 8 TMs responsible for metal coordination during transport, notably including a specific metal binding site located in TM6 with the conserved Cys-Pro-(Cys/His/Ser) motif and several other conserved residues (Argüello 2003; Pedersen et al. 2012; Hanikenne and Baurain 2014; Wang et al. 2014). Out of 45 P-type ATPases in *A. thaliana*, eight are IB metal ATPases (AtHMA1-8), which can be further divided in subgroups based on metal transport specificity (Axelsen and Palmgren 1998; Argüello 2003; Hanikenne et al. 2005; Chan et al. 2010; Pedersen et al. 2012; Hanikenne and Baurain 2014). (i) AtHMA5-AtHMA8 transport monovalent metal cations (e.g. Cu^{+}) and belong to the ubiquitous IB-1 subclass of metal ATPases found in all domains of life. This subclass includes the two human IB P-type ATPases, ATP7A and ATP7B, which both transport monovalent copper and whose mutations determine Menkes and Wilson diseases, respectively (Lutsenko and Petris 2003). In plants, the PAA1 (AtHMA6) and PAA2 (AtHMA8) proteins are responsible for copper transport across the inner envelope and thylakoid membranes, respectively, which is required for copper delivery to plastocyanin (Shikanai et al. 2003; Abdel-Ghany et al. 2005; Bernal et al. 2007). (ii) AtHMA2-4 transport divalent metal cations (e.g. Zn^{2+} and Cd^{2+}) and belong to subclass IB-2 of metal ATPases found in plants and in prokaryotes. (iii) AtHMA1 belongs to subclass IB-4 of metal ATPases and has a broad ion specificity (Ca^{2+}, Cd^{2+}, Zn^{2+}, Cu^{2+}) (Seigneurin-Berny et al. 2006; Moreno et al. 2008; Kim et al. 2009; Boutigny et al. 2014). HMA1 orthologs in plants originate from a horizontal gene transfer from Chlamydiae into the common ancestor of Plantae and all share a non-canonical Ser-Pro-Cys in TM6 (Baum 2013; Hanikenne and Baurain 2014).

IB metal ATPases possess N- and C-terminal extensions that contain high affinity metal binding domains (MBDs) rich in Cys and sometimes His residues. For instance, the C-terminal domain of AtHMA4 contains multiple di-Cys motifs and an extended His stretch. This domain may act as a zinc and cadmium sensor regulating the export capacity of the pump and is required for the full function of the protein *in planta* (Baekgaard et al. 2010; Mills et al. 2010).

The N-terminal domains of IB-1 copper ATPases are characterized by Cys-x-x-Cys motifs, which are required for copper delivery by metallochaperones, protein activation and/or protein intracellular trafficking. These processes have been described in detail for ATP7A and ATP7B (Barry et al.

2010). In contrast, the N-terminal domain of plant IB-2 zinc ATPases possess a Cys-Cys-x-x-Glu conserved metal-binding motif (CCxxE) within a βαββαβ ferredoxin fold. This non-canonical site binds one zinc atom (Eren et al. 2007; Zimmermann et al. 2009). Deletion of the AtHMA2 N-terminal domain results in decreased ATPase activity (Eren et al. 2007) and in failure to complement the phenotype of the *hma2hma4 A. thaliana* mutant (Wong et al. 2009). Mutation of the two Cys residues of the motif into Ala equally impairs the function of the protein in vivo (Wong et al. 2009). The N-terminal domain of AtHMA2 is thus essential for function *in planta*. Finally, the N-terminal domain of AtHMA4 was characterized using Nuclear Magnetic Resonance (NMR) and metal probes, which revealed zinc binding by the Cys and Glu residues of the $C^{27}CTSE^{31}$ motif and showed that its affinity for zinc was in the subnanomolar range (Zimmermann et al. 2009). The two Cys residues of the motif were required for function of AtHMA4 in yeast (Verret et al. 2005).

Conserved MBD motifs in the N-terminal domain of copper IB P-type ATPases have distinct functions in different proteins or even different functions when present in tandem in the same protein ((Tsivkovskii et al. 2001; Mana-Capelli et al. 2003; Mandal et al. 2003; Argüello et al. 2007; Veldhuis et al. 2009; Palmgren and Nissen 2011; Drees et al. 2015). It is thus important to examine differences and commonalities in the role of the N-terminal domains and their conserved MBDs for several IB P-type ATPases. Moreover, many examples exists in the literature illustrating the fact that the functional analysis of IB P-type ATPase MBDs may result in differing observations between in vivo and in vitro experiments, and also depending on the experimental setup (see for instance, Eren et al. 2007; Wong et al. 2009; Baekgaard et al. 2010; Mills et al. 2010; Drees et al. 2015). Here, to further advance our understanding of structure/function relationship in the HMA4 N-terminal domain, a range of mutants of the $C^{27}CTSE^{31}$ conserved motif were characterized by complementary in vivo and in vitro approaches. Our data highlight the key function of the domain *in planta* and reveal predominance of the two Cys residues for zinc coordination and affinity.

Materials and methods

Plant material, transformation and growth conditions

A. thaliana L. Heynhold (accession Columbia, Col-0) and the *A. thaliana hma2hma4* double mutant (Hussain et al. 2004) were used in all experiments. For genetic transformation of the *hma2hma4* mutant, plants were cultivated on soil watered with a 1 mM $ZnSO_4$ solution in a controlled climate room at 22 °C and a 8 h day^{-1} photoperiod (short days) during 8 weeks. Plants were then transferred in a 16 h day^{-1} photoperiod (long days) growth chamber to induce flowering and were watered with 3 mM $ZnSO_4$ for 5 weeks. The *hma2hma4* plants were then transformed using *Agrobacterium tumefasciens* by floral dipping (Clough and Bent 1998). GFP fusions were transformed into Col-0 wild-type plants.

For experiments, homozygous transgenic seeds (T3 generation) were germinated on 1/2 MS agar medium containing 1 % sucrose in short days, after a 5 day incubation at 4 °C. After 18 days, seedlings were transferred on soil for phenotyping or into hydroponic trays (Araponics, Tocquin et al. 2003) containing modified Hoagland solution as described (Talke et al. 2006; Charlier et al. 2015; Nouet et al. 2015). For soil experiments, plants were watered with distillated water and grown for 2 weeks in short days followed by 5 weeks in long days. For hydroponic experiments, plants were grown for 2 weeks in control conditions (1 µM $ZnSO_4$) in short days. Plants were then transferred in long days to initiate the treatments: 0.05 µM $CdSO_4$ or 0.2 µM $ZnSO_4$ (Nouet et al. 2015). Nutrient solutions were changed weekly during 4 weeks. Root and shoot samples were then harvested separately before processing for ICP-AES analyses.

Cloning

To construct the *pAtHMA4-AhHMA4* cassette and the $C^{27}CTSE^{31}$ variants, the *AtHMA4* promoter (*pAtHMA4*, 2595 bp, Hanikenne et al. 2008) was amplified from Col-0 genomic DNA by PCR using primers harbouring 5′-*Asc*I and 3′-*Acy*I restriction sites (Table S1A), respectively. The promoter fragment was cloned into the *Asc*I and *Acy*I sites of a *pAhHMA4-1-AhHMA4* pBluescript II KS + vector (Hanikenne et al. 2008) in replacement of *pAhHMA4-1*. This vector served as a template for the site-directed mutagenesis of the conserved N-terminal $C^{27}CTSE^{31}$ motif as described (Talke et al. 2006) using mutagenic primers (Table S1B). The wild-type and variant versions of *pAtHMA4-AhHMA4* were then excised by digestion with *Asc*I and *Pac*I and cloned at the corresponding sites of a promoter-less variant of the pMDC32 vector (Curtis and Grossniklaus 2003; Hanikenne et al. 2008).

For localization experiments, the wild-type and variant versions of *AhHMA4* were cloned at the *Pac*I and *Asc*I sites (Table S1A) in fusion with GFP into the pMDC83 vector allowing expression under the control of a double 35S promoter (Curtis and Grossniklaus 2003).

For production in *E. coli*, a synthetic gene encoding the N-terminal part of the *A. halleri* HMA4 protein (AhHMA4n, residues 1–95) with optimized codon usage was

obtained from GeneArt. The fragment was subsequently cloned into the pET9a expression vector (Novagen) using *Nde*I and *Bam*HI restriction sites. Variants with mutations in the $C^{27}CTSE^{31}$ motif were obtained as above using the pET9a-AhHMA4n vector as template (see mutagenic primers in Table S1B).

All final constructions were verified by sequencing.

RNA extraction, cDNA synthesis, and quantitative RT-PCR

Total RNAs were prepared using the RNeasy Plant Mini kit with on column DNAse treatment (Qiagen), and cDNAs were synthesized using the RevertAid H Minus First Strand cDNA Synthesis kit with Oligo dT (Thermo Scientific). Transcript levels were determined by real-time RT-PCR in 384-well plates with an ABI Prism 7900HT system (Applied Biosystems) using MESA GREEN qPCR MasterMix (Eurogentec) as described (Talke et al. 2006; Nouet et al. 2015) including 4 technical replicates for each sample/primer pair (Online Resource 2). The quality of the PCRs was checked visually through analysis of dissociation and amplification curves. Relative gene expression levels were determined by normalization using multiple reference genes with the qBase software (Biogazelle, Hellemans et al. 2007). Three reference genes (At1g18050, *UBQ10, EF1a*) were selected from the literature (Czechowski et al. 2005). Their adequacy to normalize gene expression in our experimental conditions was verified using the geNorm software in qBase (gene stability measure $M = 0.404$, pairwise variation $CV = 0.155$) (Vandesompele et al. 2002).

ICP-AES analyses

For plant samples, shoot tissues were rinsed in milliQ water, whereas root tissues were desorbed and washed as described (Talke et al. 2006). Tissues were then dried at 60 °C for 2 days. For protein samples, proteins were dialyzed against the purification buffer A without zinc (see below). Samples (10–50 mg of tissues, 5–10 µM purified proteins) were then acid-digested in DigiPrep tubes with 3 ml ≥65 % (w/w) HNO_3 (Sigma-Aldrich) on a DigiPrep Graphite Block Digestion System (SCP Science) as follows: 15 min at 45 °C, 15 min at 65 °C and 90 min at 105 °C. After cooling, sample volumes were adjusted to 10 ml with milliQ water and 200 µl ≥65 % HNO_3 (Sigma-Aldrich). Metal concentrations were determined by ICP-AES (Inductively Coupled Plasma-Atomic Emission Spectroscopy, Vista AX, Varian).

GFP imaging

Leaves of eighteen day-old T1 seedlings expressing the GFP fusions described above were analyzed (3 independent lines per construct). Images were collected using a SP2 inverted confocal microscope (Leica). An Argon/Ion laser (488 nm) was used for excitation of the GFP protein and the emission light was dispersed and recorded at 500–540 nm, as described (Rausin et al. 2010). To induce plasmolysis, seedlings were incubated in a 6 % (w/v) NaCl solution for 5 min prior observation.

Production and purification of non-labelled and isotope-labelled N-terminal domains

E. coli cells [strain BL21 (DE3)] transformed with the pET9a/AhHMA4n expression vector were grown at 37 °C in 2 l of LB (Luria–Bertani) medium containing 50 µM $ZnCl_2$ and 50 µg/ml kanamycin. At an OD_{600} of ~0.8, the production was directly induced with 1 mM IPTG (isopropyl β-D-thiogalactopyranoside). The culture was then incubated for 18 h at 18 °C. The cells, collected by centrifugation, were resuspended in 50 ml of 10 mM Tris/HCl pH 8 supplemented by 1 mM TCEP and 50 µM $ZnCl_2$ (buffer A). A protease inhibitor cocktail (mini complete EDTA-free, Roche) was added to avoid the degradation of the protein.

For isotope labelling, prior induction of expression, cells were harvested an OD_{600} of ~0.8 by centrifugation at 11,000*g* for 20 min and resuspended in 500 ml of M9 medium containing $[^{15}N]NH_4Cl$ and/or $[^{13}C]$Glucose (Cambridge Isotope Labotaries, Inc.), 50 µM $ZnCl_2$ and 50 µg/ml kanamycin. After 1 h incubation at 37 °C, the expression of the protein was induced by 1 mM IPTG. Labelled proteins were then collected as described above.

In all cases, cells were lysed after harvest using an EmulsiFlex-C3 cell disrupter (Avestin). The cellular extracts were clarified by centrifugation at 48,000*g* for 40 min at 4 °C. The soluble fraction was then loaded onto a cation exchange Sepharose column (24 ml, GE Healthcare) equilibrated in 10 mM Tris/HCl pH 8 supplemented with 1 mM TCEP and 50 µM $ZnCl_2$. The bound proteins were eluted over a 250 ml linear NaCl gradient (0–300 mM). The fractions containing AhHMA4n were pooled, dialyzed overnight against buffer A (see above) and then further purified on a 5 ml Poros HS column (Applied Biosystems). The proteins were eluted thanks to a linear NaCl gradient as above.

The N-terminal domain variants were purified as described for the native AhHMA4 N-terminal domain. However, for variants $C^{27}A$, $C^{28}A$ and $C^{27}A/C^{28}A/E^{31}A$, purification conditions were slightly different: (i) 10 mM Tris/HCl pH 8, 1 mM TCEP, 50 µM $ZnCl_2$ and 0.02 % n-Dodecyl β-D-Maltopyranoside was used for equilibration and (ii) the elution gradient was increased to 1 M NaCl.

The AhHMA4n fractions were concentrated by ultrafiltration on a 3 kDa molecular-mass cut-off column

(Vivaspin). The protein purity was assessed by SDS/PAGE (18 % gels), and the final protein concentration was determined by using the molar absorption coefficient at 280 nm ($\varepsilon = 8480\ M^{-1}\ cm^{-1}$), which was calculated with the help of ProtParam (ExPASy Proteomics Server, http://expasy.org/).

Determination of the affinity of HMA4n for zinc

The AtHMA4n control was produced as reported previously (Zimmermann et al. 2009). The oxidised AhHMA4n protein with an internal disulphide bond (i.e. AhHMA4n-SS) was produced by quantitative oxidation of AhHMA4n with stoichiometric amount of $[Fe^{III}(CN)_6]^{3+}$ and purified by an ion-exchange column. The AhHMA4n native and variant proteins were produced as described above. To ensure a complete removal of all metal ions from the samples, they were incubated with excess EDTA, followed by a gel-filtration separation.

The determination of zinc (Zn^{II}) affinity was conducted via the competition reaction 1 and the data analysed via Eq. 2 (Xiao et al. 2013):

$$[Zn^{II}(Par)_2] + P \rightleftharpoons Zn^{II}\text{-}P + 2Par\ K_{ex} \quad (P = \text{protein or EGTA}) \tag{1}$$

$$\frac{[P]_{tot}}{[Zn]_{tot}} = K_D\beta_2\left(\frac{[Par]_{tot}}{[Zn^{II}(Par)_2]} - 2\right)^2[Zn^{II}(Par)_2] \times \left(1 - \frac{[Zn^{II}(Par)_2]}{[Zn]_{tot}}\right) + 1 - \frac{[Zn^{II}(Par)_2]}{[Zn]_{tot}} \tag{2}$$

The term $[Zn^{II}(Par)_2]$ is the equilibrium concentration of probe complex $[Zn^{II}(Par)_2]$ in Eq. 1 and may be determined directly from the solution absorbance at 500 nm after subtracting the minor contribution from the Par ligand. The other terms in Eq. 2 are the known total concentrations of the relevant species. The term K_D $\beta_2 = (K_{ex})^{-1}$ is a constant under fixed conditions and may be derived by curve-fitting of the experimental data to Eq. 2. However, the accumulated formation constant β_2 for $Zn^{II}(Par)_2$ varies considerably with experimental conditions and this will affect the reliability of K_D for Zn^{II}-P (Zimmermann et al. 2009). To control such variation, the EGTA ligand, whose affinities for Zn^{II} at various pH values are known, was used as a control affinity calibrator under each experimental condition. Consequently, the K_D for Zn^{II}-P may be obtained reliably via Eq. 3 relative to a control experiment in the same reaction medium with P = EGTA in Eq. 1:

$$K_D(Zn^{II}\text{-}P) = [K_{ex}(EGTA)/K_{ex}(P)] \times K_D(Zn^{II}\text{-}EGTA) \tag{3}$$

The experiments were conducted in MOPS buffer (50 mM, pH 7.3, 100 mM NaCl) with the detailed procedure following that reported previously (Zimmermann et al. 2009). To ensure a complete reduction of all protein thiols, reductant TCEP (100 μM) was included in all reaction media (except for the experiments with the oxidised HMA4n sample). Control experiments showed that excess TCEP had no discernible impact on the estimated Zn(II) affinity.

Nuclear magnetic resonance analysis

The spectral assignment experiment of the native and $C^{27}A/C^{28}A/E^{31}A$ triple mutant HMA4n domains were performed on 0.5 mM ^{13}C- and ^{15}N-labelled samples while the HSQC experiments on the single mutants ($C^{27}A$, $C^{28}A$ and $E^{31}A$) were conducted on 0.07–0.14 mM ^{15}N-labelled samples. The apo form of AhHMA4n was obtained by treating 100 μM of protein with 400 μM EDTA for 10 min. All samples were prepared in a buffer containing 10 mM NH_4Ac, 1 mM TCEP, 100 mM NaCl at pH 6.6 with 5 % D_2O and DSS 10 μM. The different spectra were acquired at 293 K on a Bruker AVI 500 MHz spectrometer equipped with a TCI cryogenically cooled probe. The spectra of the 2D (^1H–^{15}N HSQC) and 3D [HNCA, HNCO, HNCACB and CBCA(CO)NH] (Cavanagh et al. 1996) experiments were processed using TOPSPIN (Bruker) and analyzed with CCPNmr.

NMR minimum chemical shift perturbation

The effects of N-terminal domain mutations on the amide NH resonances were analysed as follows. For each cross-peak in the 1H–15 N HSQC spectrum of the wild-type protein, the nearest cross-peak (in terms of 1H and 15 N chemical shifts) in the spectrum of each mutant was identified. The 1H and 15 N chemical shift differences, ΔH and ΔN, between each such pair of cross-peaks were measured and used to calculate a "minimum Chemical Shift Perturbation" (mCSP) (Lian et al. 2000).

$$mCSP = \sqrt{(6.7\Delta H)^2 + \Delta N^2}$$

While the individual chemical shifts may be underestimated, the perturbed amide NH can be reliably identified (Williamson et al. 1997). The minimum chemical shift is plotted as a function of residue number. The calculations were performed using TOPSPIN (*xpk) peak lists and a custom made tcl script.

A threshold value was estimated in order to determine significant CSP. In a first step, all CSP are considered and the average ($\langle CSP \rangle$) plus three times the standard deviation (σ) is calculated. Then, the highest CSP ($CSP \geq \langle CSP \rangle + 3\sigma$) are removed from the data and new average

and new standard deviation are calculated. The operation is repeated until convergence is reached. The final value $\langle CSP \rangle + 3\sigma$ for the residues not significantly perturbed corresponds to the threshold (Tavel et al. 2012).

Statistical analysis

All statistical analyses of the data were carried out using STATISTICA (Statsoft).

Results

In this study, we selected the *A. halleri* HMA4 protein as an experimental system to examine in vivo and in vitro the function of the conserved N-terminal $C^{27}CTSE^{31}$ metal binding motif. The AtHMA4 and AhHMA4 protein share 96.8 % identity over the 95 residue N-terminal domain (Online Resource 1).

The $C^{27}CTSE^{31}$ motif of the N-terminal domain is essential for the function of the HMA4 protein in vivo

To examine in vivo the function of the $C^{27}CTSE^{31}$ N-terminal motif of HMA4 (Zimmermann et al. 2009), we separately mutated the two Cys and the Glu residues into Ala. A triple mutant, where the two Cys and the Glu were mutated into Ala, was also generated (Fig. 1a). The native (*AhHMA4*) and mutated genes were expressed under the control of the endogenous *A. thaliana HMA4* promoter (pAtHMA4) in the loss-of-function *hma2hma4 A. thaliana* mutant (Hussain et al. 2004). Several independent homozygous transgenic lines (T3 generation) were obtained for each construct. The *HMA4* gene variants were expressed at similar levels in plant tissues (Online Resource 2).

In our growth conditions on standard soil watered with tap water, the expression of *AhHMA4* rescued the phenotype of the *hma2hma4* mutant. The plants developed normally and were able to flower and set seeds without additional zinc supply in the soil, as Col-0 wild-type plants (Fig. 1b–e). In contrast, expression of the $C^{27}CTSE^{31}$ motif variants resulted in the absence of ($C^{27}A$, $C^{28}A$, triple mutant) or in partial ($E^{31}A$) complementation, respectively (Fig. 1f–j). Indeed, plant expressing the $C^{27}A$, $C^{28}A$ and triple mutants displayed the stunted growth and chlorotic phenotype typical of the *hma2hma4* mutant (Hussain et al. 2004; Wong and Cobbett 2009; Mills et al. 2010). These plants could complete their life cycle and set seeds only upon massive external zinc supply. The plants expressing the $E^{31}A$ mutant presented a phenotype intermediate between Col-0 and *hma2hma4* plants, with a larger rosette

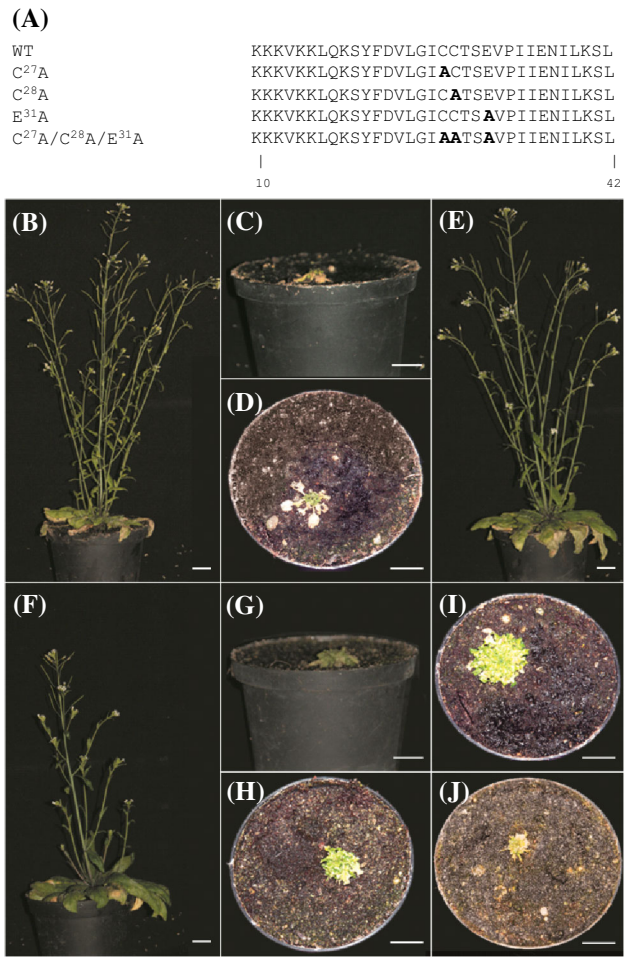

Fig. 1 Complementation of the *hma2hma4 A. thaliana* mutant by the *A. halleri* HMA4 protein and $C^{27}CTSE^{31}$ variants expressed under the control of the *pAtHMA4* promoter. **a** Partial sequences of the AhHMA4 N-terminal (AhHMA4n) domain. Mutated residues in the $C^{27}CTSE^{31}$ motif are shown in bold font. **b–j** Phenotype of the plants after 8 weeks of growth on standard soil. Plants were grown without Zn supplementation for phenotyping. Wild-type *A. thaliana* plants (Col-0 accession) (**b**) and the *hma2hma4* mutant (**c–d**) are shown as controls. Mutant plants expressing a native AhHMA4 protein (**e**) or $C^{27}A$ (**g–h**), $C^{28}A$ (**i**), $E^{31}A$ (**f**) and triple $C^{27}A/C^{28}A/E^{31}A$ (**j**) variants display wild-type (**e**) or mutant phenotypes (**g-j**). *Scalebars* 1 cm

and the development of flowers (Fig. 1f). The plants however required additional zinc supply to complete their life cycle. Note that similar results were obtained upon expression of the variants under the control of the *A. halleri HMA4-1* promoter (data not shown, Hanikenne et al. 2008).

Mutations in the $C^{27}CTSE^{31}$ motif alter zinc and cadmium distribution in plant tissues

We next determined if the mutation in the $C^{27}CTSE^{31}$ motif altered metal accumulation in plant tissues. Zinc and cadmium concentrations were measured by ICP-AES in roots and rosette leaves of 8 week old wild-type (Col-0)

and *hma2hma4* plants as well as transgenic plants expressing the $C^{27}CTSE^{31}$ variants after cultivation for four weeks in Hoagland hydroponic medium containing either 0.2 µM Zn or 0.05 µM Cd (Nouet et al. 2015). The *hma2hma4* mutant accumulated about sixfold higher zinc and fourfold higher cadmium in roots and 2.2-fold lower zinc and sixfold lower cadmium in shoots than the wild-type, respectively (Fig. 2). This reflected the inability of the *hma2hma4* mutant to translocate zinc and cadmium from root to shoot. Expression of the native *AhHMA4* gene in the *hma2hma4* genetic background almost completely restored wild-type levels of zinc accumulation in root and shoot tissues. The plants expressing the $C^{27}A$, $C^{28}A$ and triple mutants accumulated zinc at levels identical to the *hma2hma4* mutant. In contrast, expression of the $E^{31}A$ mutant partially restored shoot zinc accumulation to levels intermediate between Col-0 and the *hma2hma4* mutant, but only marginally reduced root accumulation (Fig. 2a, b). Identical observations were made upon 0.05 µM Cd exposure (in the presence of 1 µM Zn): only the expression of the $E^{31}A$ mutant resulted in moderate increase of cadmium accumulation in shoots compared to the *hma2hma4* mutant (Fig. 2c, d).

The $C^{27}CTSE^{31}$ motif is not required for plasma membrane localization

Mutations in the N-terminal domain of AhHMA4 might impact its intracellular localization. The inability of the $C^{27}CTSE^{31}$ motif variants to complement the phenotype of the *hma2hma4* mutant may therefore results from a mis-localization of the protein in cells rather than a loss of function. To exclude this hypothesis and to ascertain that the variants are expressed at the protein level, we expressed GFP fusions of the $C^{27}CTSE^{31}$ AhHMA4 variants under the control of a double 35S promoter in the Col-0 genetic background.

Leaves of 18-day-old seedlings expressing the GFP fusions were imaged by confocal microscopy. All three simple mutants ($C^{27}A$, $C^{28}A$ and $E^{31}A$) and the triple mutant of the AhHMA4 protein were expressed and localized in the plasma membrane of leaf epidermal cells

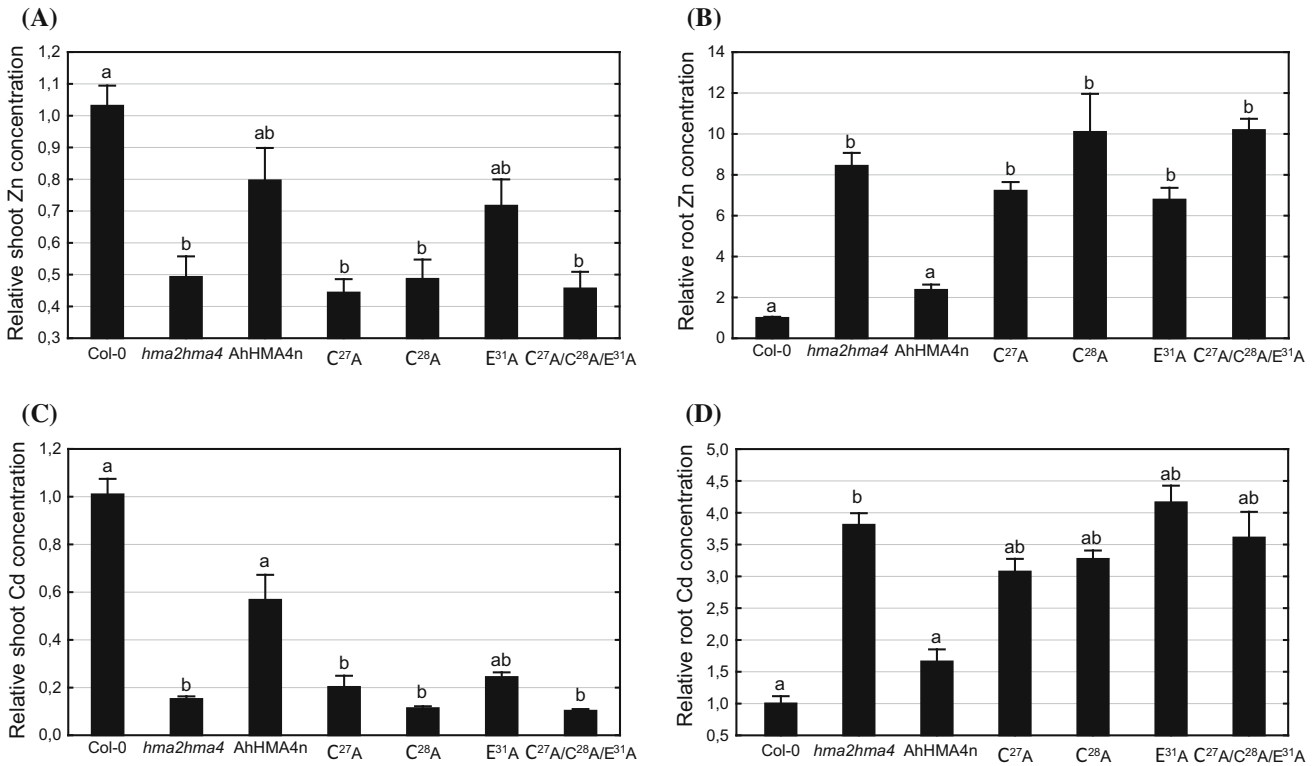

Fig. 2 Zinc and cadmium accumulation in plants expressing AhHMA4n variants. Wild-type *A. thaliana* plants (Col-0 accession), *hma2hma4* mutant and mutant plants expressing a native AhHMA4 protein or $C^{27}A$, $C^{28}A$, $E^{31}A$ and triple $C^{27}A/C^{28}A/E^{31}A$ variants were grown for 4 weeks in Hoagland hydroponic medium containing 0.2 µM $ZnSO_4$ (**a**, **b**) or 0.05 µM $CdSO_4$ (**c**, **d**). Metal contents (mg kg^{-1} DW) were measured by ICP-AES from root and shoot tissues. Values relative to the wild-type (Col-0) are mean ± SEM of 2-3 independent lines from two independent experiments, each including two replicates of 3 plants per line. The data were analyzed with a Kruskal–Wallis non-parametric ANOVA followed by multiple comparison tests. Statistically significant differences ($p < 0.01$) between means are indicated by different superscripted letters

(Fig. 3). The induction of a plasmolysis of leaf cells confirmed the plasma membrane localization of the protein: a characteristic detachment of the membrane from the cell-wall, with the exception of plasmodesmata, was observed (Fig. 3f). No fluorescence was detected in leaves of Col-0 seedlings using identical settings (Fig. 3a). GFP imaging experiments also suggests that the $C^{27}CTSE^{31}$ motif variant proteins are stable *in planta*, as we did not detect any GFP aggregation in cells (Fig. 3).

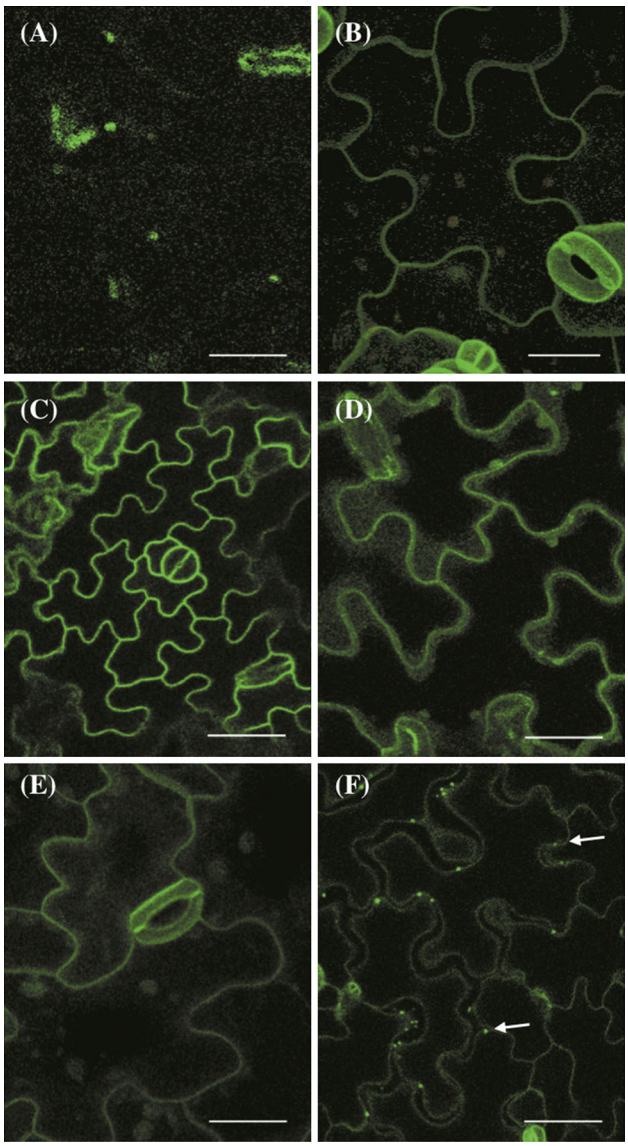

Fig. 3 Cellular localization of $C^{27}CTSE^{31}$ AhHMA4 variants. GFP fusions of $C^{27}A$ (**b**), C28A (**c**), $E^{31}A$ (**d**) and triple $C^{27}A/C^{28}A/E^{31}A$ (**e**) variants were imaged by confocal microscopy in leaves of 18 day-old seedlings. The fusions were expressed in the Col-0 background under the control of a double 35S promoter. Non transformed Col-0 seedlings served as controls (**a**). **f** Plasmolysis on leaf of AhHMA4 $C^{28}A$ expressing plants confirmed plasma membrane localization. The *arrow* indicates a plasmodesmata. *Scalebars* 20 μM

Mutations in the $C^{27}CTSE^{31}$ motif alter zinc binding properties in vitro

The native N-terminal domain of AhHMA4 (residues 1–95 residues, AhHMA4n) and the $C^{27}CTSE^{31}$ variants were expressed in *E. coli* and purified. After dialysis, we assessed the stoichiometry of zinc binding to the proteins by ICP-AES measurements (Table 1). The native AhHMA4n bound ~1 zinc ion per protein. Zinc binding was strongly reduced for the $C^{27}A$ and $C^{28}A$ mutant proteins as well as for the triple mutant. The $E^{31}A$ mutant retained an intermediate zinc binding capacity (Table 1).

Using the Par zinc probe (Zimmermann et al. 2009), we next quantitatively estimated the binding affinity of the AhHMA4n variants for zinc (Table 2 and Online Resource 3). The native AhHMA4n protein had a K_D for zinc in the nanomolar range identical to that for the AtHMA4n protein (previously determined by Zimmermann et al. 2009), despite 3 polymorphic positions in the N-terminal domain (see Online Resource 1). Oxidation of the two Cys thiols to an internal disulfide bond in the binding motif completely abolished zinc binding. The $C^{27}A$ mutation, taken as a representative of the most affected mutant variants, decreased affinity for zinc by 1.8 orders of magnitude, whereas the $E^{31}A$ mutation only reduced the affinity for zinc by 1.4 orders of magnitude.

Structural impact of the $C^{27}CTSE^{31}$ motif mutations by NMR spectroscopy

To examine the structural consequences of mutations in the $C^{27}CTSE^{31}$ motif of AhHMA4, 2D 15N–1H HSQC NMR experiments were recorded for the native and $C^{27}CTSE^{31}$ variant AhHMA4n proteins. Backbone NH NMR signal chemical shifts and intensities are very sensitive probes to study protein structural and dynamic modifications. The HSQC spectrum of the native AhHMA4n protein was similar to previously published data for AtHMA4n (Zimmermann et al. 2009). The HSQC spectra of the $C^{27}CTSE^{31}$ motif variants revealed that the AhHMA4n domains were structured, despite (strongly) reduced zinc binding capability (Table 1), and displayed limited

Table 1 Stoechiometry of zinc binding to AhHMA4 $C^{27}CTSE^{31}$ N-terminal variants

	Ratio Zn/protein
AhHMA4n	0.86
AhHMA4n $C^{27}A$	0.06
AhHMA4n $C^{28}A$	<0.01
AhHMA4n $E^{31}A$	0.37
AhHMA4n $C^{27}A/C^{28}A/E^{31}A$	<0.01

Table 2 Affinity of zinc binding to AhHMA4 $C^{27}CTSE^{31}$ N-terminal variants

Protein	log K_D^a ([Par]$_{tot}$, 50 μM)	log K_D^a ([Par]$_{tot}$, 100 μM)	Average log K_D	log [K_D/K_D(wt)]
AtHMA4n[b]	<−9.40[a]	−9.63	−9.63	~0
AhHMA4n	<−9.47[a]	−9.60	−9.60	0
AhHMA4n $C^{27}A$	−7.82	−7.83	−7.83	1.8
AhHMA4n $E^{31}A$	−8.21	−8.19	−8.20	1.4
AhHMA4n SS	ND[c]			

[a] The affinity for zinc was determined at two Par concentrations (50 and 100 μM) (see Zimmermann et al. 2009)

[b] Used as control (described in Zimmermann et al. 2009)

[c] Not detectable

variations compared to the spectrum of the native AhHMA4n domain (Fig. 4 and Online Resource 4). These observations suggested that mutations in the $C^{27}CTSE^{31}$ motif had limited impact on the domain structure. To statistically support these conclusions, an analysis of the minimal chemical shift perturbations (mCSP) was used to compare the HSQC spectra of the native and $C^{27}CTSE^{31}$ variant AhHMA4n proteins (Fig. 5a, Online Resource 5). The observed mCSPs corresponded to the mutated amino acid residues and to amino acid residues interacting with the mutated residues (Fig. 5). A very similar mCSP profile was also obtained for the apo form of the protein obtained by treatment with EDTA prior to NMR analysis (Online Resource 6).

Backbone assignment (N, H, CO, Ca, Cb) was performed for the native AhHMA4n protein and the triple $C^{27}A/C^{28}A/E^{31}A$ mutant, which represented the most extreme modification of the $C^{27}CTSE^{31}$ motif. This confirmed that perturbed amino acid residues are located at the vicinity of the zinc binding site or correspond to more distant residues in the primary sequence that are spatially close in the 3D structure. Structure predictions using the backbone chemical shift and the Talos$^+$ software (Shen et al. 2009) confirmed that the mutations in the $C^{27}CTSE^{31}$

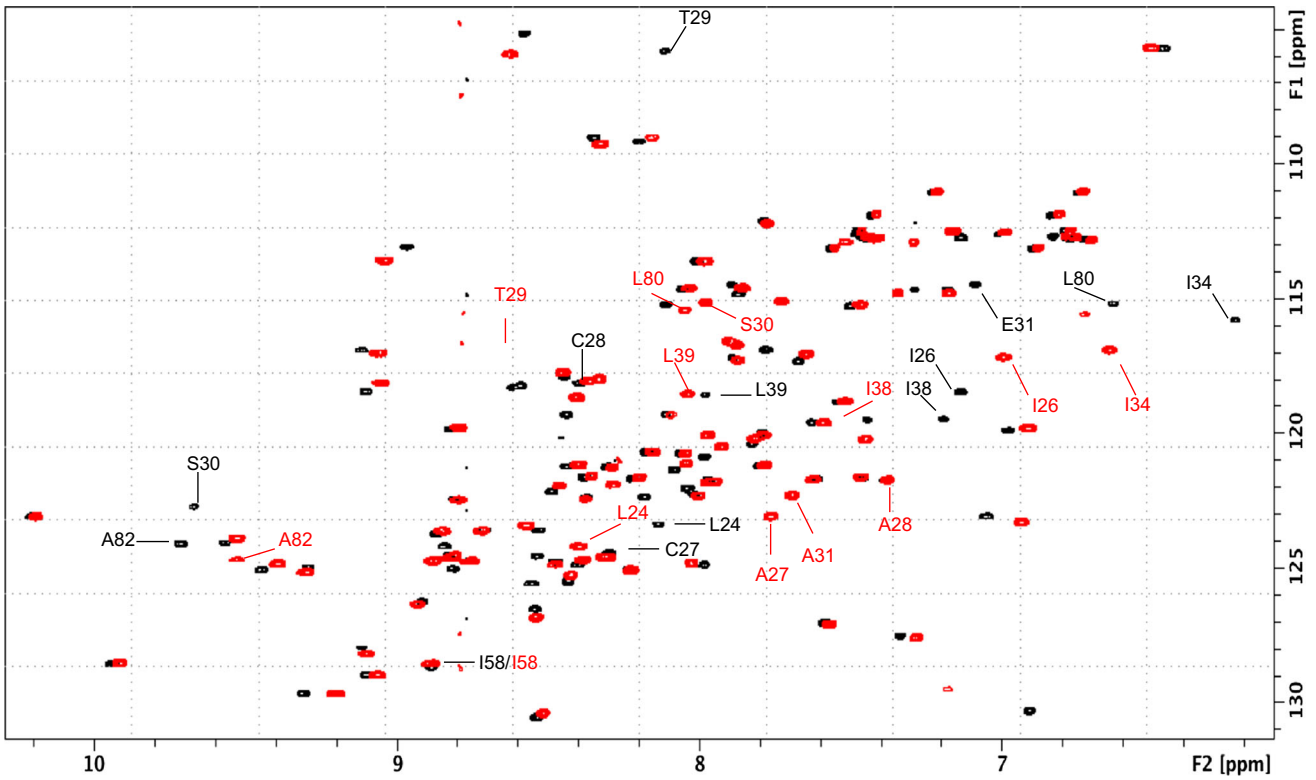

Fig. 4 Superposition of the 2D HSQC ^1H-^{15}N NMR spectra of the native (in *black*) and triple $C^{27}A/C^{28}A/E^{31}A$ mutant (in *red*) AhHMA4n proteins at pH 6.6. The marked peaks (*arrows*) represent the most affected residues

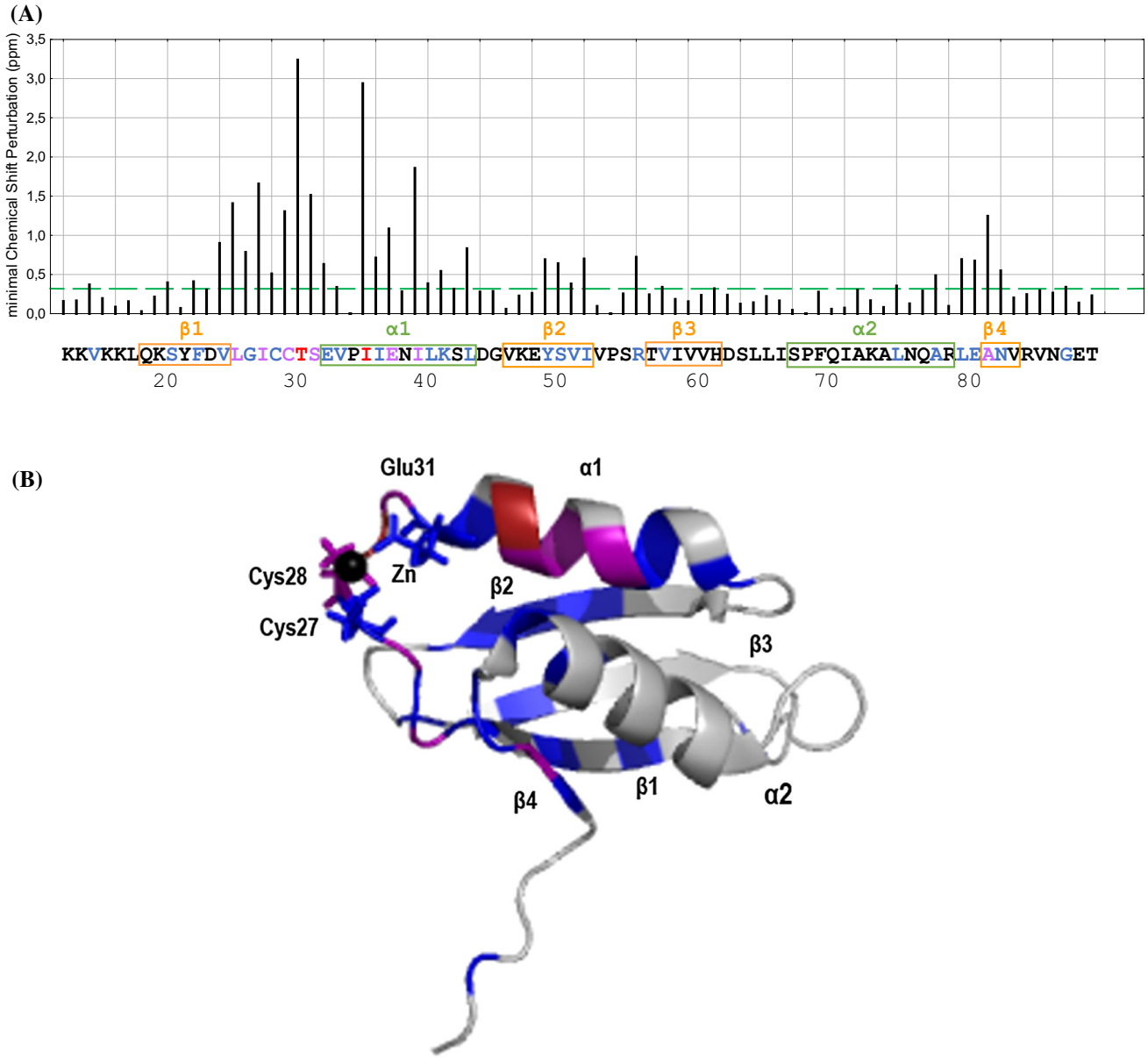

Fig. 5 Chemical shift perturbation resulting from the $C^{27}A/C^{28}A/E^{31}A$ mutation in the AhHMA4n protein. **a** A threshold of 3 standard deviations (*green line*) was selected to identify significant shift perturbations when comparing the native and triple $C^{27}A/C^{28}A/E^{31}A$ mutant AhHMA4n proteins. The *green* and *orange boxes* represent the alpha helices and beta sheets in the sequence, respectively. **b** The shift perturbations were localized on the structure of AtHMA4n [2KKH (Zimmermann et al. 2009)] using Pymol. A color code for residues was used to represent the level of perturbation: *red* $\geq$ 2 ppm; 2 ppm $\leq$ *purple* $\leq$ 1 ppm; *blue* $\leq$ 1 ppm

motif did not have a major impact on the AhHMA4n domain secondary structure (data not shown).

Discussion

IB P-type ATPase proteins play essential roles in metal homeostasis in *Arabidopsis* species (Williams and Mills 2005; Nouet et al. 2011). Hence, HMA4 is a major actor in Zn hyperaccumulation as well as Zn and Cd tolerance in *Arabidopsis halleri* (Talke et al. 2006; Courbot et al. 2007; Willems et al. 2007; Hanikenne et al. 2008, 2013). If the catalytic mechanism of transport by P-type ATPases is well described, establishing the roles and functions of N- and C-terminal extremities and their MBDs still require further investigations. Depending on the organisms and proteins, N-terminal MBDs have been involved in multiple functions, including regulatory roles, controlling catalytic activities, dephosphorylation and metal ion release possibly via interactions with the cytoplasmic ATP binding domain,

or the intracellular targeting of the protein (Tsivkovskii et al. 2001; Mana-Capelli et al. 2003; Mandal et al. 2003; Argüello et al. 2007; Veldhuis et al. 2009).

Zimmermann et al. (2009) determined the 3D solution structure of the N-terminal domain of AtHMA4, which binds one zinc atom at the $C^{27}CTSE^{31}$ motif. Here, we examined the function of this motif *in planta*, assessed the contribution of the conserved Cys and Glu residues to zinc binding and evaluated the impact of mutations in the motif on protein structure and function. Combining both in vivo and in vitro analyses allowed an integrated analysis of the structure/function relationship for the N-terminal MBD of HMA4.

The HMA4 protein localizes to the plasma membrane in plant tissues (Verret et al. 2004; Courbot et al. 2007; Siemianowski et al. 2013; Nouet et al. 2015). The N-terminal domain of HMA4 was not involved in protein intracellular localization or in protein stability (Fig. 3). Indeed, all mutant variants in fusion with GFP localized in the plasma membrane of stable *A. thaliana* transformants (Fig. 3), in agreement with previous results for AtHMA2 (Wong et al. 2009). In contrast, the C-terminal domain of AtHMA2 possibly contains a signal important for the subcellular localization of the protein *in planta* (Wong et al. 2009), whereas the C-terminal domain of AtHMA4 is not required for correct localization in yeast cells (Baekgaard et al. 2010).

Expression of the *AhHMA4* gene under the control of the pAtHMA4 promoter only partially complemented the defect in root to shoot zinc translocation of the *hma2hma4* mutant: zinc shoot accumulation level was lower than in the wild-type, but was however sufficient to sustain normal development (Figs. 1, 2). When expressed under the control in the *HMA4* endogenous promoter, *HMA4* is thus not sufficient alone to fully compensate for the loss of both *HMA2* and *HMA4*. In contrast, expressing the same gene under the control of promoters of the *A. halleri HMA4*, which are stronger than the pAtHMA4 promoter (Hanikenne et al. 2008) fully complemented the mutant (Nouet et al. 2015).

In complementation experiments, the $C^{27}A$, $C^{28}A$ and $C^{27}A/C^{28}A/E^{31}A$ mutations abolished the ability of the AhHMA4 protein to complement the strong zinc deficiency phenotype and to restore zinc and cadmium root-to-shoot translocation in the *hma2hma4 A. thaliana* mutant (Figs. 1, 2). Reduced zinc binding and affinity (Tables 1, 2, Online Resource 3) are thus accompanied by a loss of function *in planta*. Previous studies analysing the N-terminal MDB of AtHMA2 ($\sim$82 % sequence identity with the AtHMA4 N-terminal domain, see Online Resource 1) suggested that the CCxxE motif is required for zinc and cadmium binding in vitro and for maximum enzyme turnover but were not essential for activity or metal binding to transmembrane metal binding sites in yeast cells (Eren et al. 2007). However, the two Cys residues of the motif were required for function of AtHMA2 *in planta* (Wong et al. 2009) and AtHMA4 in yeast (Verret et al. 2005).

In contrast, the $E^{31}A$ mutation sustained partial complementation of the *hma2hma4* mutant phenotype (Figs. 1, 2) and retained higher zinc binding and affinity than the Cys→Ala mutants (Tables 1, 2, Online Resource 3). Note that this mutant retained a higher capacity for zinc translocation to the shoot than for cadmium (Fig. 2).

The NMR HSQC spectrum of the amide NHs of the purified AhHMA4n protein was nearly identical to the data obtained by Zimmermann et al. (2009) for AtHMA4n. Since NMR chemical shifts are very sensitive to the structural environment, the very similar NMR spectrum was a strong evidence for a very similar 3D structure. This confirmed the global ferredoxin βαββαβ fold of the domain, in which the thiols of Cys residues and carboxy group of the Glu residue contributed to the coordination of zinc. The three polymorphic residues between AtHMA4n and AhHMA4n had thus no major impact on protein structure. Furthermore, we showed here that the mutations in the $C^{27}CTSE^{31}$ motif of AhHMA4n, which drastically reduced zinc binding, had no significant effect either on the secondary or on the tertiary structure of the protein. This observation was also confirmed by the structural analysis of the apo form of AhHMA4n: the structure of the apo form is not altered.

Altogether, our data indicated that the two Cys residues of the $C^{27}CTSE^{31}$ motif of the N-terminal MBD are essential for the function of HMA4, whereas the Glu residue is important but not essential. Moreover, zinc binding to the N-terminal MBD is crucial for HMA4 protein function, whereas it is not required to maintain the N-terminal domain structure. Based on these observations arises the following question: what is the requirement of zinc binding for the protein function? It may be required for intramolecular interactions controlling the pump's activity and/or conformational changes during metal transport (Tsivkovskii et al. 2001).

Copper IB pType ATPases and many bacterial zinc IB pType ATPases possess a highly conserved CxxC motif in their N-terminal MDBs. This motif can bind both monovalent (Cu^{+}) or divalent (Cu^{2+}, Zn^{2+}, Cd^{2+}) metal ions in vitro and, for instance, metal selectivity for Cu^{+} is determined in vivo by electrostatic and hydrophobic interactions with specific copper chaperones (Argüello et al. 2007). However, in all plant zinc IB pType ATPases, this conserved motif is replaced by a CCxxE motif. It was initially suggested that the CCxxE motif could confer selectivity for Zn(II) but not for Cu(I) due to its higher binding affinity for Zn(II) than for Cu(I) (Eren et al. 2007). However, this conclusion has been questioned when both

CCxxE and CxxC motifs were showed to bind Cu(I) with affinities at least 6 orders of magnitude higher than Zn(II). Both motifs can also bind Zn(II) with moderate affinities in the nanomolar range (Zimmermann et al. 2009). Quantitative evaluations under identical conditions revealed that the MBDs containing the CCxxE motif bind Zn(II) with affinities 20–30 times stronger than do those MBDs containing CxxC while relative affinities for Cu(I) are inverted by a factor of 30–50 (Zimmermann et al. 2009). Consequently, it was proposed that, under metal-limiting conditions, zinc selectivity is conferred by relative affinities and not absolute affinities. Under these conditions, Cu(I) ions are confined to their native high affinity sites and are not available to compete for native Zn(II) sites (Zimmermann et al. 2009). Interestingly, the affinity for zinc of the $E^{31}A$ domain of HMA4 featuring a CCxxA metal binding motif is essentially identical to that of the N-terminal domain of the copper ATPase HMA7 containing a CxxC metal binding motif (Zimmermann et al. 2009). Yet, in the *hma2hma4 A. thaliana* mutant, the endogenous copper ATPases, such as HMA5 (Andrés-Colás et al. 2006; Kobayashi et al. 2008) or HMA7, do not seem to substitute HMA2 and HMA4 for Zn/Cd transport while the AhHMA4 $E^{31}A$ variant did partially sustain the Zn/Cd transport function. It appears that the functional specificity of different metal transporters must also depend on factors other than the metal-binding affinity and that these may include specific intra-molecular interactions (Tsivkovskii et al. 2001) or expression patterns. Interestingly, bacterial zinc (ZntA) and cadmium (CadA) IB pType ATPases also use a carboxylate ligand for zinc and cadmium, respectively, with the presence of a DCxxC motif found in the *E. coli* ZntA and of a Glu residue in a loop more distant of the CxxC motif in the CadA N-terminal domain (Banci et al. 2002; 2006).

In conclusion, our analyses highlight the importance of zinc binding to the N-terminal MBD of HMA4 for the protein function *in planta*. This work further establishes the value of combining *in planta* and in vitro studies to reveal the structure/function relationships for transmembrane metal transporters. Future developments may possibly include analysing the interaction of the N-terminal domain and its MBD variants with other cytoplasmic domains of HMA4.

Acknowledgments We thank Dr. C. Nouet, S. Fanara, M. Schloesser and M.C. Requier for technical support. Prof. A. Wedd is thanked for his constructive comments and suggestions. We thank Dr. M. Haydon for the kind gift of *hma2hma4* seeds. Funding was provided by the "Fonds de la Recherche Scientifique–FNRS" (FRFC-2.4583.08, PDR-T.0206.13) (MH, MG), the University of Liège (SFRD-12/03) (MH), the Belgian Program on Interuniversity Poles of Attraction (IAP no. P6/19) and the Australian Research Council (Grant DP130100728) (AAU, ZX). MH is Research Associate of the FNRS. Doctoral fellowships were funded by the FNRS (CL) and the "Fonds pour la formation à la Recherche dans l'Industrie et dans l'Agriculture" (GL, JBC).

Author contribution MG and MH conceived and directed the study. MH, MG, CD and ZX designed experiments. CL, GL, JBC, BB, AAU, ZX and CD performed experiments. CL, MH, CD, GL, BB, AAU and ZX analysed the data. MH, MG, CD, AAU, ZX, PM and MC contributed reagents/materials/analysis tools. MH, CL and MG wrote the paper and all authors commented on the manuscript.

References

Abdel-Ghany SE, Müller-Moulé P, Niyogi KK, Pilon M, Shikanai T (2005) Two P-type ATPases are required for copper delivery in Arabidopsis thaliana chloroplasts. Plant Cell 17:1233–1251. doi:10.1105/tpc.104.030452

Andrés-Colás N et al (2006) The Arabidopsis heavy metal P-type ATPase HMA5 interacts with metallochaperones and functions in copper detoxification of roots. Plant J 45:225–236

Argüello JM (2003) Identification of ion-selectivity determinants in heavy-metal transport P1B-type ATPases. J Membr Biol 195:93–108

Argüello JM, Eren E, Gonzàlez-Guerrero M (2007) The structure and function of heavy metal transport P1B-ATPases. Biometals 20:233–248. doi:10.1007/s10534-006-9055-6

Axelsen KB, Palmgren MG (1998) Evolution of substrate specificities in the P-Type ATPase superfamily. J Mol Evol 46:84–101. doi:10.1007/pl00006286

Baekgaard L et al (2010) A combined zinc/cadmium sensor and zinc/cadmium export regulator in a heavy metal pump. J Biol Chem 285:31243–31252. doi:10.1074/jbc.M110.111260

Banci L, Bertini I, Ciofi-Baffoni S, Finney LA, Outten CE, O'Halloran TV (2002) A new Zinc–protein coordination site in intracellular metal trafficking: solution structure of the Apo and Zn(II) forms of ZntA(46–118). J Mol Biol 323:883–897. doi:10.1016/S0022-2836(02)01007-0

Banci L et al (2006) Structural basis for metal binding specificity: the N-terminal cadmium binding domain of the P1-type ATPase CadA. J Mol Biol 356:638–650. doi:10.1016/j.jmb.2005.11.055

Barry AN, Shinde U, Lutsenko S (2010) Structural organization of human Cu-transporting ATPases: learning from building blocks. J Biol Inorg Chem 15:47–59. doi:10.1007/s00775-009-0595-4

Baum D (2013) The origin of primary plastids: a pas de deux or a ménage à trois? Plant Cell 25:4–6. doi:10.1105/tpc.113.109496

Bernal M, Testillano PS, Alfonso M, del Carmen Risueño M, Picorel R, Yruela I (2007) Identification and subcellular localization of the soybean copper P1B-ATPase GmHMA8 transporter. J Struct Biol 158:46–58. doi:10.1016/j.jsb.2006.10.016

Boutigny S et al (2014) HMA1 and PAA1, two chloroplast-envelope PIB-ATPases, play distinct roles in chloroplast copper homeostasis. J Exp Bot 65:1529–1540. doi:10.1093/jxb/eru020

Broadley MR, White PJ, Hammond JP, Zelko I, Lux A (2007) Zinc in plants. New Phytol 173:677–702

Cavanagh J, Fairbrother WE, Palmer AG III, Skelton NJ (1996) Protein NMR Spectroscopy Principles and Practice. San Diego

Chan H et al (2010) The p-type ATPase superfamily. J Mol Microbiol Biotechnol 19:5–104. doi:10.1159/000319588

Charlier JB et al (2015) Zinc triggers a complex transcriptional and post-transcriptional regulation of the metal homeostasis gene *FRD3* in *Arabidopsis* relatives. J Exp Bot 66:3865–3878. doi:10.1093/jxb/erv188

Clough SJ, Bent AF (1998) Floral dip: a simplified method forAgrobacterium-mediated transformation of *Arabidopsis thaliana*. Plant J 16:735–743. doi:10.1046/j.1365-313x.1998.00343.x

Courbot M, Willems G, Motte P, Arvidsson S, Roosens N, Saumitou-Laprade P, Verbruggen N (2007) A major quantitative trait locus for cadmium tolerance in Arabidopsis halleri colocalizes with HMA4, a gene encoding a heavy metal ATPase. Plant Physiol 144:1052–1065. doi:10.1104/pp.106.095133

Craciun AR, Meyer C-L, Chen J, Roosens N, De Groodt R, Hilson P, Verbruggen N (2012) Variation in *HMA4* gene copy number and expression among *Noccaea caerulescens* populations presenting different levels of Cd tolerance and accumulation. J Exp Bot 63:4179–4189. doi:10.1093/jxb/ers104

Cun P et al (2014) Modulation of Zn/Cd P(1B2)-ATPase activities in Arabidopsis impacts differently on Zn and Cd contents in shoots and seeds. Metallomics 6:2109–2116. doi:10.1039/c4mt00182f

Curtis MD, Grossniklaus U (2003) A gateway cloning vector set for high-throughput functional analysis of genes in planta. Plant Physiol 133:462–469

Czechowski T, Stitt M, Altmann T, Udvardi MK, Scheible WR (2005) Genome-wide identification and testing of superior reference genes for transcript normalization in Arabidopsis. Plant Physiol 139:5–17

Drees SL, Beyer DF, Lenders-Lomscher C, Lübben M (2015) Distinct functions of serial metal-binding domains in the *Escherichia coli* P1B-ATPase CopA. Mol Microbiol 97:423–438. doi:10.1111/mmi.13038

Eren E, González-Guerrero M, Kaufman BM, Argüello JM (2007) Novel Zn^{2+} coordination by the regulatory N-terminus metal binding domain of *Arabidopsis thaliana* Zn($^{2+}$)-ATPase HMA2. Biochemistry 46:7754–7764. doi:10.1021/bi7001345

Gaither LA, Eide DJ (2001) Eukaryotic zinc transporters and their regulation. Biometals 14:251–270

Goyer RA (1997) Toxic and essential metal interactions. Annu Rev Nutr 17:37–50

Hall JL, Williams LE (2003) Transition metal transporters in plants. J Exp Bot 54:2601–2613. doi:10.1093/jxb/erg303

Hanikenne M, Baurain D (2014) Origin and evolution of metal P-type ATPases in Plantae (Archaeplastida). Front Plant Sci 4:544. doi:10.3389/fpls.2013.00544

Hanikenne M, Nouet C (2011) Metal hyperaccumulation and hypertolerance: a model for plant evolutionary genomics. Curr Opin Plant Biol 14:252–259

Hanikenne M, Krämer U, Demoulin V, Baurain D (2005) A comparative inventory of metal transporters in the green alga *Chlamydomonas reinhardtii* and the red alga *Cyanidioschizon merolae*. Plant Physiol 137:428–446. doi:10.1104/pp.104.054189

Hanikenne M et al (2008) Evolution of metal hyperaccumulation required *cis*-regulatory changes and triplication of *HMA4*. Nature 453:391–395. doi:10.1038/nature06877

Hanikenne M, Kroymann J, Trampczynska A, Bernal M, Motte P, Clemens S, Krämer U (2013) Hard selective sweep and ectopic gene conversion in a gene cluster affording environmental adaptation. PLoS Genet 9:1–13

Hellemans J, Mortier G, De Paepe A, Speleman F, Vandesompele J (2007) qBase relative quantification framework and software for management and automated analysis of real-time quantitative PCR data. Genome Biol 8:R19

Hussain D et al (2004) P-type ATPase heavy metal transporters with roles in essential zinc homeostasis in Arabidopsis. Plant Cell 16:1327–1339. doi:10.1105/tpc.020487

Kim YY, Choi H, Segami S, Cho HT, Martinoia E, Maeshima M, Lee Y (2009) AtHMA1 contributes to the detoxification of excess Zn(II) in Arabidopsis. Plant J 58:737–753. doi:10.1111/j.1365-313X.2009.03818.x

Kobayashi Y et al (2008) Amino acid polymorphisms in strictly conserved domains of a P-Type ATPase HMA5 are involved in the mechanism of copper tolerance variation in arabidopsis. Plant Physiol 148:969–980

Krämer U (2010) Metal hyperaccumulation in plants. Annu Rev Plant Biol 61:517–534. doi:10.1146/annurev-arplant-042809-112156

Krämer U, Talke IN, Hanikenne M (2007) Transition metal transport. FEBS Lett 581:2263–2272. doi:10.1016/j.febslet.2007.04.010

Kühlbrandt W (2004) Biology, structure and mechanism of P-type ATPases. Nat Rev Mol Cell Biol 5:282–295. doi:10.1038/nrm1354

Lian L-Y et al (2000) Mapping the binding site for the GTP-binding protein Rac-1 on its inhibitor RhoGDI-1. Structure 8:47–56. doi:10.1016/S0969-2126(00)00080-0

Lutsenko S, Petris MJ (2003) Function and regulation of the mammalian copper-transporting ATPases: insights from biochemical and cell biological approaches. J Membr Biol 191:1–12

Mana-Capelli S, Mandal AK, Argüello JM (2003) *Archaeoglobus fulgidus* CopB is a thermophilic Cu^{2+}-ATPase: functional role of its histidine-rich-N-terminal metal binding domain. J Biol Chem 278:40534–40541. doi:10.1074/jbc.M306907200

Mandal AK, Mikhailova L, Argüello JM (2003) The Na, K-ATPase S5–H5 helix: structural link between phosphorylation and cation-binding sites. Ann N Y Acad Sci 986:224–225

Mills RF, Krijger GC, Baccarini PJ, Hall JL, Williams LE (2003) Functional expression of AtHMA4, a P1B-type ATPase of the Zn/Co/Cd/Pb subclass. Plant J 35:164–176

Mills RF, Valdes B, Duke M, Peaston KA, Lahner B, Salt DE, Williams LE (2010) Functional significance of AtHMA4 C-terminal domain in planta. PLoS ONE 5:e13388. doi:10.1371/journal.pone.0013388

Moreno I et al (2008) AtHMA1 is a thapsigargin sensitive Ca^{2+}/heavy metal pump. J Biol Chem 283:9633–9641

Nouet C, Motte P, Hanikenne M (2011) Chloroplastic and mitochondrial metal homeostasis. Trends Plant Sci 16:395–404. doi:10.1016/j.tplants.2011.03.005

Nouet C, Charlier JB, Carnol M, Bosman B, Farnir F, Motte P, Hanikenne M (2015) Functional analysis of the three *HMA4* copies of the metal hyperaccumulator *Arabidopsis halleri*. J Exp Bot 66:5783–5795. doi:10.1093/jxb/erv280

O'Lochlainn S et al (2011) Tandem Quadruplication of *HMA4* in the Zinc (Zn) and Cadmium (Cd) Hyperaccumulator *Noccaea caerulescens*. PLoS ONE 6:e17814

Palmer CM, Guerinot ML (2009) Facing the challenges of Cu, Fe and Zn homeostasis in plants. Nat Chem Biol 5:333–340

Palmgren MG, Nissen P (2011) P-type ATPases. Annu Rev Biophys 40:243–266. doi:10.1146/annurev.biophys.093008.131331

Pedersen CNS, Axelsen KB, Harper JF, Palmgren MG (2012) Evolution of plant P-type ATPases. Front Plant Sci 3:31. doi:10.3389/fpls.2012.00031

Rausin G, Tillemans V, Stankovic N, Hanikenne M, Motte P (2010) Dynamic nucleocytoplasmic shuttling of an Arabidopsis SR splicing factor: role of the RNA-binding domains. Plant Physiol 153:273–284. doi:10.1104/pp.110.154740

Seigneurin-Berny D et al (2006) HMA1, a new Cu-ATPase of the chloroplast envelope, is essential for growth under adverse light conditions. J Biol Chem 281:2882–2892. doi:10.1074/jbc.M508333200

Shen Y, Delaglio F, Cornilescu G, Bax A (2009) TALOS+: a hybrid method for predicting protein backbone torsion angles from NMR chemical shifts. J Biomol NMR 44:213–223. doi:10.1007/s10858-009-9333-z

Shikanai T, Müller-Moulé P, Munekage Y, Niyogi KK, Pilon M (2003) PAA1, a P-type ATPase of Arabidopsis, functions in copper transport in chloroplasts. Plant Cell 15:1333–1346

Siemianowski O, Barabasz A, Weremczuk A, Ruszczyńska A, Bulska EWA, Williams LE, Antosiewicz DM (2013) Development of Zn-related necrosis in tobacco is enhanced by expressing AtHMA4 and depends on the apoplastic Zn levels. Plant, Cell Environ 36:1093–1104. doi:10.1111/pce.12041

Talke IN, Hanikenne M, Krämer U (2006) Zinc-dependent global transcriptional control, transcriptional deregulation, and higher gene copy number for genes in metal homeostasis of the hyperaccumulator *Arabidopsis halleri*. Plant Physiol 142:148–167. doi:10.1104/pp.105.076232

Tavel L et al (2012) Ligand binding study of human PEBP1/RKIP: interaction with nucleotides and Raf-1 peptides evidenced by NMR and mass spectrometry. PLoS ONE 7:e36187. doi:10.1371/journal.pone.0036187

Tocquin P, Corbesier L, Havelange A, Pieltain A, Kurtem E, Bernier G, Périlleux C (2003) A novel high efficiency, low maintenance, hydroponic system for synchronous growth and flowering of Arabidopsis thaliana. BMC Plant Biol 3:2

Toyoshima C (2008) Structural aspects of ion pumping by Ca^{2+}-ATPase of sarcoplasmic reticulum. Arch Biochem Biophys 476:3–11. doi:10.1016/j.abb.2008.04.017

Toyoshima C (2009) How Ca^{2+}-ATPase pumps ions across the sarcoplasmic reticulum membrane. Biochim Biophys Acta 1793:941–946. doi:10.1016/j.bbamcr.2008.10.008

Toyoshima C, Inesi G (2004) Structural basis of ion pumping by Ca^{2+}-ATPase of the sarcoplasmic reticulum. Annu Rev Biochem 73:269–292. doi:10.1146/annurev.biochem.73.011303.073700

Toyoshima C, Nomura H (2002) Structural changes in the calcium pump accompanying the dissociation of calcium. Nature 418:605–611. doi:10.1038/nature00944

Tsivkovskii R, MacArthur BC, Lutsenko S (2001) The Lys 1010-Lys1325 fragment of the Wilson's disease protein binds nucleotides and interacts with the N-terminal domain of this protein in a copper-dependent manner. J Biol Chem 276:2234–2242. doi:10.1074/jbc.M003238200

Tuerk MJ, Fazel N (2009) Zinc deficiency. Curr Opin Gastroenterol 25:136–143. doi:10.1097/MOG.0b013e328321b395

Vandesompele J, De Preter K, Pattyn F, Poppe B, Van Roy N, De Paepe A, Speleman F (2002) Accurate normalization of real-time quantitative RT-PCR data by geometric averaging of multiple internal control genes. Genome Biol 3:RESEARCH0034

Veldhuis N, Gaeth A, Pearson R, Gabriel K, Camakaris J (2009) The multi-layered regulation of copper translocating P-type ATPases. Biometals 22:177–190. doi:10.1007/s10534-008-9183-2

Verret F et al (2004) Overexpression of AtHMA4 enhances root-to-shoot translocation of zinc and cadmium and plant metal tolerance. FEBS Lett 576:306–312

Verret F, Gravot A, Auroy P, Preveral S, Forestier C, Vavasseur A, Richaud P (2005) Heavy metal transport by AtHMA4 involves the N-terminal degenerated metal binding domain and the C-terminal His11 stretch. FEBS Lett 579:1515–1522

Wang K et al (2014) Structure and mechanism of Zn^{2+}-transporting P-type ATPases. Nature 514:518–522. doi:10.1038/nature13618

Willems G, Drager DB, Courbot M, Gode C, Verbruggen N, Saumitou-Laprade P (2007) The genetic basis of zinc tolerance in the metallophyte *Arabidopsis halleri* ssp. *halleri* (Brassicaceae): an analysis of quantitative trait loci. Genetics 176:659–674. doi:10.1534/genetics.106.064485

Williams LE, Mills RF (2005) P(1B)-ATPases–an ancient family of transition metal pumps with diverse functions in plants. Trends Plant Sci 10:491–502. doi:10.1016/j.tplants.2005.08.008

Williamson RA, Carr MD, Frenkiel TA, Feeney J, Freedman RB (1997) Mapping the binding site for matrix metalloproteinase on the N-terminal domain of the tissue inhibitor of metalloproteinases-2 by NMR chemical shift perturbation. Biochemistry 36:13882–13889. doi:10.1021/bi9712091

Wong CK, Cobbett CS (2009) HMA P-type ATPases are the major mechanism for root-to-shoot Cd translocation in Arabidopsis thaliana. New Phytol 181:71–78. doi:10.1111/j.1469-8137.2008.02638.x

Wong CK, Jarvis RS, Sherson SM, Cobbett CS (2009) Functional analysis of the heavy metal binding domains of the Zn/Cd-transporting ATPase, HMA2, in *Arabidopsis thaliana*. New Phytol 181:79–88. doi:10.1111/j.1469-8137.2008.02637.x

Xiao Z, Gottschlich L, van der Meulen R, Udagedara SR, Wedd AG (2013) Evaluation of quantitative probes for weaker Cu(I) binding sites completes a set of four capable of detecting Cu(I) affinities from nanomolar to attomolar. Metallomics 5:501–513. doi:10.1039/c3mt00032j

Zimmermann M et al (2009) Metal binding affinities of Arabidopsis zinc and copper transporters: selectivities match the relative, but not the absolute, affinities of their amino-terminal domains. Biochemistry 48:11640–11654. doi:10.1021/bi901573b